# Imaging brain microstructure: an overview of diffusion MR method development at PIFa/CFIN

Brian Hansen[1] and Sune N. Jespersen[1,2]
[1]: CFIN, Aarhus University, Denmark
[2]: Dept. of Physics and Astronomy, Aarhus University, Denmark

## Introduction:

Brain microstructure is a key part of brain function. For instance normal brain function relies on the brain's ability to adabt structurally to experience. Similarly, when disease affects brain microstructure, function suffers. Therefore, MR imaging methods to assess tissue microstructure would be of great value in the study of normal brain function as well as in diagnostics of a host of diseases such as Alzheimer's, stress, depression, and alcoholism to name a few.

The neurophysics group uses biophysical modelling and MRI data to develop methods to study the brain's microstructure. For this work the newly established high field MRI lab is an indispensable tool.

## Imaging of neurite density:

Biophysical modeling of diffusion enables estimation of tissue microstructural features such as neurite density and architecture.

The figure illustrates the idea behind the biophysical model of diffusion in gray matter presented in [1,2]. This approach enables measurements of neurite density (volume fraction of cylinders).

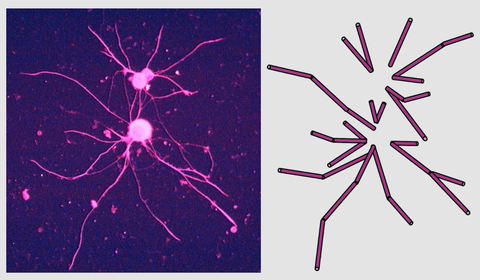

$$S/S_0 = (1-\nu)\exp(-\mathbf{b}:\mathbf{D}_E) + \nu S_c(\mathbf{b}; D_L, D_T, fODF)$$

$\nu$ neurite density; $\mathbf{D}_E$ extracellular diffusion tensor; $S_c$ signal from neurites, longitudinal and tranverse diffusivities $D_L$ and $D_T$ and fODF.

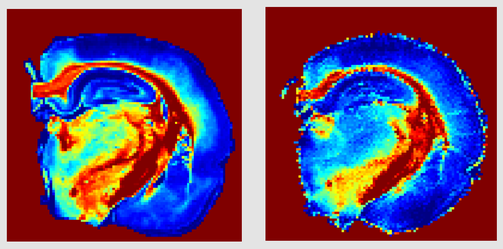

Comparison of modeled neurite density (left) and histology (right) in fixated rat brain hemispheres. Warm colors correspond to high values of neurite density/ optical staining intensity.

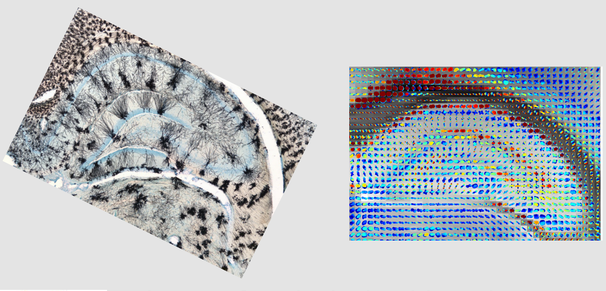

Comparison of Golgi stain histology (left) and MRI based dendrite architecture (right), i.e. the fiber orientation distribution function. One clearly recognizes the appropriate rendering of orientations in the corpus callosum, the stratum radiatum, and the absence of anisotropy in the cell layers.

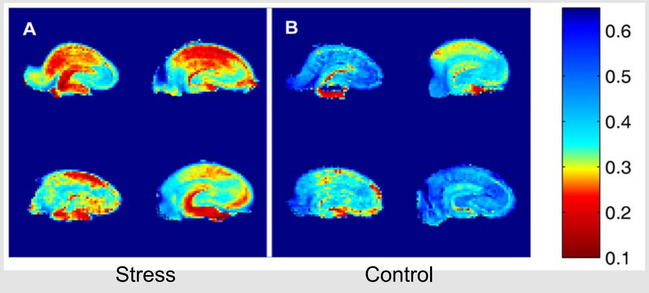


Loss of apical dendrites in various regions of the hippocampus is known histologically to be one of several pathological changes following mental stress. It is possible to detect this with modeling-based diffusion MRI: in the figure we see neurite density maps of stressed and normal rat hippocampus [3].

## Microstructural diffusion modeling also informs DTI interpretation:

$$\nu(D_L - D_T)(\mathbf{T} - \mathrm{Tr}(\mathbf{T})\mathbf{I}/3) = \mathbf{D} - \mathrm{Tr}(\mathbf{D})\mathbf{I}/3$$

**T** scatter matrix from fODF

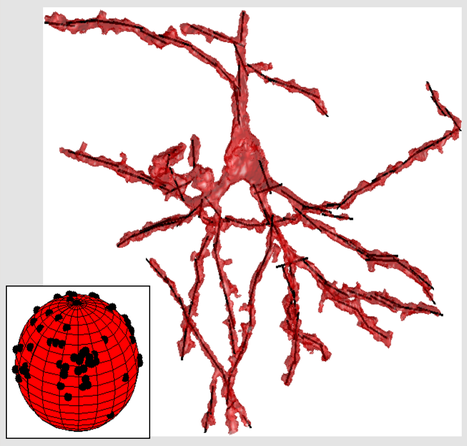

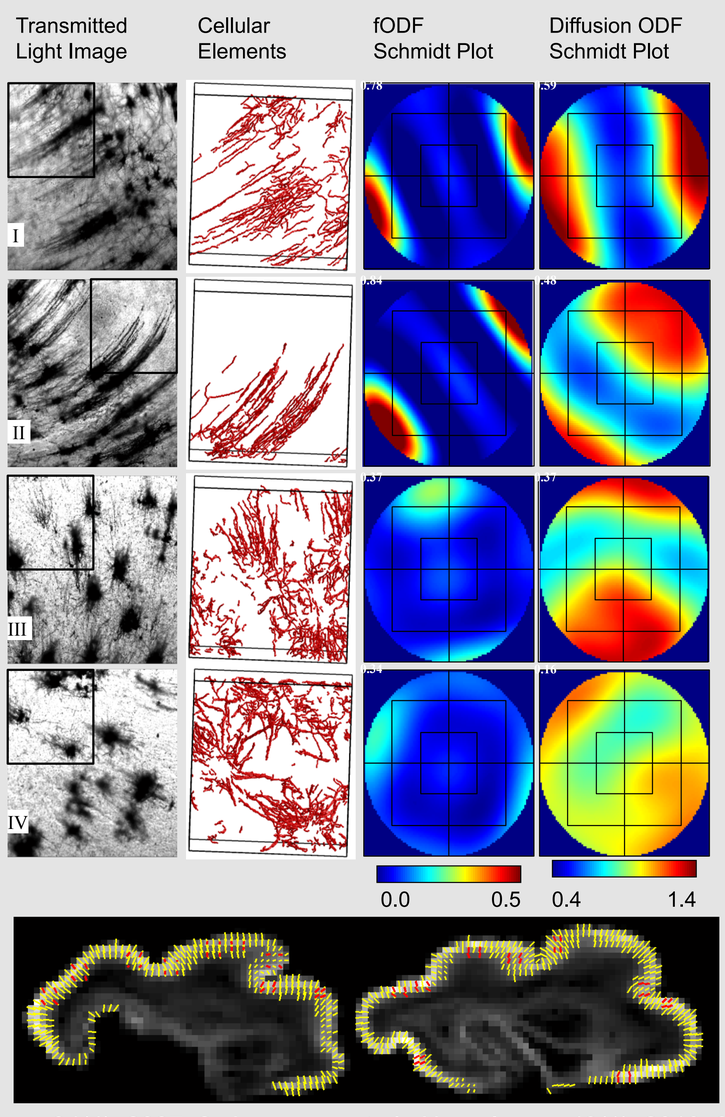


Above: Example of procedure to quantify neurite architecture based on Golgi stains of cortical neurons in the ferret. The scatter matrix is estimated from the orientations of the line elements indicated in the figure.

Right: comparison of orientation distribution of neurites to diffusion anisotropy [4].

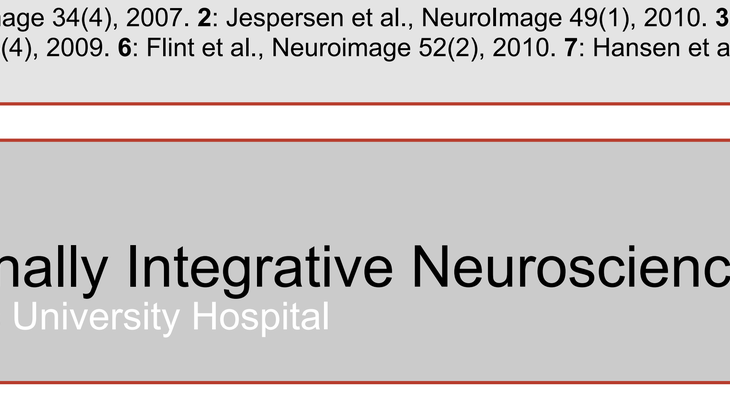

Demonstration of alignment between principal directions of neurites and diffusion tensor [4].

## Direct MR-microscopy (collaboration with the Blackband lab, UFL):

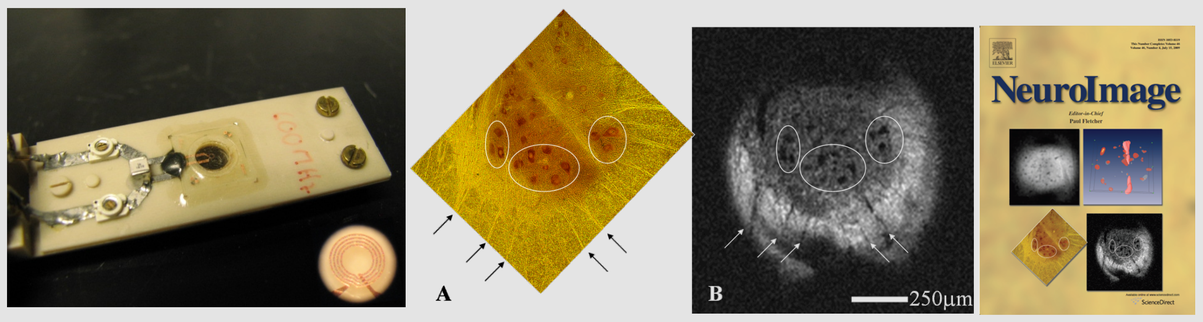


Above, left to right: An example of a micro surface coil suitable for MR microscopy with direct comparison to histology as demonstrated in [5]. The data shows the worlds first direct MR imaging of cell bodies in situ. The cells imaged are alpha-motor neurons in rat spinal cord. Axon bundles are also clearly visible.

Comparison between tractography based on diffusion tensor microscopy and histology. This study used rat and pig tissue [6].

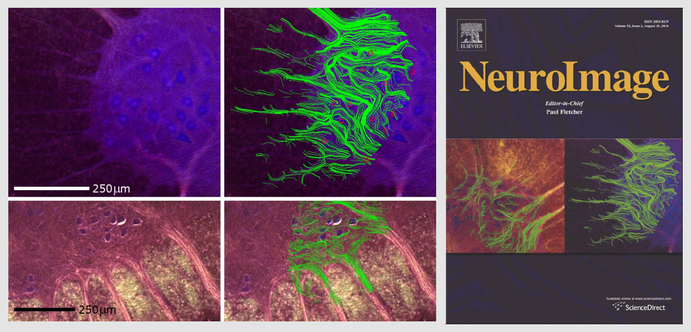


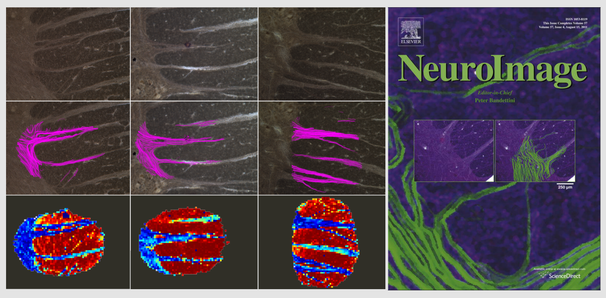


Further comparison between tractography based on diffusion tensor microscopy and histology. This study used human spinal cord and gave a quantitative comparison of tractography and histology [7].

More advanced pulse sequences can be used to extract novel information about tissue microstructure. Below are examples from fixed vervet monkey brains using double pulsed field gradient sequences [8].

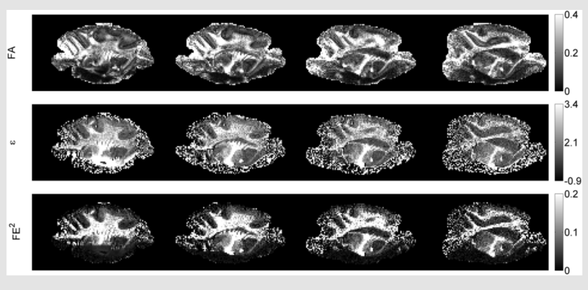


Maps of microscopic fractional eccentricity (FE) also called microscopic fractional anisotropy (μFA) [9]. Reflects fractional anisotropy of individual cells. Note areas of low FA and high μFA in both white and gray matter: this can be explained by e.g. fiber dispersion.

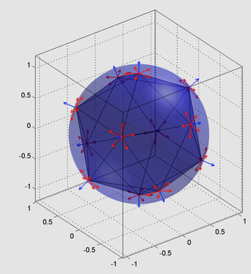

Sampling scheme for rotationally invariant μFA measurements.

## Microstructural diffusion underpinnings of diffusion kurtosis imaging:

Compared to the diffusion coefficient the microstructural underpinnings of kurtosis are quite complex:

$$\mathrm{W} = 3\nu\left[D_A^2\mathrm{U} + (1-\nu)\,sym\left((\mathrm{D}_E - D_T\mathrm{I} - D_A\mathrm{T})^{\otimes 2}\right)\right] \Big/ \mathrm{Tr}(\mathrm{D}/3)^2$$

$$U_{ijkl} = \langle n_i n_j n_k n_l\rangle - \frac{1}{3}\left(\langle n_i n_j\rangle\langle n_k n_l\rangle + \langle n_i n_k\rangle\langle n_j n_l\rangle + \langle n_i n_l\rangle\langle n_k n_j\rangle\right) \qquad sym(\mathrm{A})_{ijkl} = \frac{1}{\|P\|}\sum_{\sigma\in P} A_{\sigma(ijkl)}$$

Nevertheless, mean kurtosis is clearly affected by microstructure, has demonstrated utility as a biomarker, and can be acquired in approximately one minute [10].



Fast kurtosis sampling scheme




$\overline{W}$ from full tensor.
Scan time: ~11 mins
CPU time: ~1 hour to fit

$\overline{W}_{139}$ from fast protocol
Scan time: 55 secs
CPU time: 2 secs (whole brain)
Clinically feasible.

Mean kurtosis is considered a general microstructural marker and has proven utility in research and diagnosis of e.g. ischemia, epilepsy, gliomas, Parkinson's disease, and traumatic brain injury. The fast method presented [10] is underway as a WIP sequence for Siemens MRI systems (Jürgen Finsterbusch, Hamburg).

**References:** **1**: Jespersen et al., NeuroImage 34(4), 2007. **2**: Jespersen et al., NeuroImage 49(1), 2010. **3**: Vestergaard-Poulsen et al., PLoS ONE 6(7):e20653, 2011. **4**: Jespersen et al., IEEE Trans Med Imag 31(1), 2012. **5**: Flint et al., Neuroimage 46(4), 2009. **6**: Flint et al., Neuroimage 52(2), 2010. **7**: Hansen et al., Neuroimage 57(4), 2011. **8**: NMR in Biomedicine 26, 2013. **9**: Lasic et al., Frontiers in Physics 2014;2. **10**: Hansen et al., MRM 69, 2013.